Spectroscopic studies of the unique yellow supergiant α Aqr in the Cepheid instability strip

By: I. A. Usenko, A.S. Miroshnichenko, S. Danford

Usenko, I.A., Miroshnichenko, A.S. & Danford, S. (2017) Spectroscopic studies of the unique yellow supergiant α Aqr in the Cepheid instability strip. *Astronomy Letter*, 43(11), 751-767. doi: 10.1134/S1063773717110068

Made available courtesy of Springer: http://dx.doi.org/10.1134/S1063773717110068

Abstract:

Based on 21 spectra with resolutions from 12 000 to 42 000 taken in 1997–2016 for the yellow supergiant α Aqr (which is believed to be nonvariable in the Cepheid instability strip), we have determined its effective temperature T^{eff} and radial velocities from metal and hydrogen absorption lines. Blue and red components that account for 20–25% of the total number of lines used have been detected in the profiles of these lines. The effective temperature and radial velocities estimated from metal lines and their components do not show any noticeable variations, while the radial velocities determined from hydrogen lines show variations that are largest for the Hα line, with an amplitude of more than 10 km s^{-1}. These variations resemble periodic (~100 days) and sporadic ones. The presence of variable red components in the hydrogen line cores confirms that there is a circumstellar envelope around the supergiant. The radial velocities of these components exhibit a behavior similar to that of the hydrogen lines but with larger amplitudes (it is twice that for the R component of the Hα line). Such an unusual variability as well as the presence of blue components in metal lines and the star's position at the red edge of the Cepheid instability strip can be explained by a possible residual pulsational activity in the upper atmospheric layers of the star, which "swings" the envelope with a larger amplitude when passing into a less dense medium. The multicomponent structure of the Na I D doublet lines and their variations over long time intervals may be indicative of a chromospheric activity and a change in the stellar wind intensity. These processes can affect the sporadic variations of the radial velocities in the upper atmospheric layers of the star and its envelope. We raise the question about a revision of the classification of α Aqr as a yellow nonvariable supergiant.

Keywords: yellow supergiants | Cepheid instability strip | spectra | radial velocities | hydrogen absorption lines | circumstellar envelopes | small-amplitude pulsations

Article:

INTRODUCTION

The star α Aqr is a unique object. As a yellow G2 Ib supergiant (Keenan and McNeil 1989), this star is near the red edge of the Cepheid instability strip (CIS) for fundamental-mode pulsators (Usenko 2017) and is the only representative of its class that has a so-called hybrid chromosphere. In addition, the object enters into the list of so-called nonvariable supergiants in the CIS, the Fernie–Hube–Schmidt list (Fernie and Hube 1971; Schmidt 1972). As a bright star (mV = 2m. 94), it is often used as a spectroscopic standard.

Physical Properties

Spectroscopic studies of the supergiant revealed emission in the Ca II H and K lines (Wilson and Bappu 1957). Subsequently, its significant variations were observed for several days: strong in the K component and weak in the H component (Hollans and Beebe 1976). The Na I, Ca II H and K, and Al II lines were found to be blueshifted by 25 km s^{-1} (Dupree 1986). Based on the spectrum taken on July 1, 1993, Usenko (2017) estimated this shift for the Na I D lines to be 3.9 and 1.8 km s−1, respectively. Multiple observations from the IUE satellite revealed emission in the Mg II h and k lines with an asymmetry, suggesting a *chromospheric mass loss* (Stencel and Mullan 1980). As Mullan and Stencel (1982) showed, the variability in the Mg II h and k lines is discrete. Hartmann et al. (1982) detected coronal emission in the He II 1640 ˚A line, suggesting the presence of a *strong stellar wind*. The detection of short-wavelength emission lines of carbon, oxygen, silicon, sulfur neutral atoms as well as helium, magnesium, and calcium mentioned above (Reimers 1982) led to the conclusion that the supergiant has the above-mentioned hybrid chromosphere with a solar-type transition region (where most of the emissions are formed) and a cool part (where the absorptions in a strong high-velocity (more than 100 km s^{-1}) stellar wind are formed). Furthermore, variations in the intensity of emission lines with a period of 900d–1000d were observed (Oznovich and Gibson 1987). In 1979 O'Brien and Lambert (1986) detected emission in the He II 10 830 Å line, with the absorption component being blueshifted by 200 km s−1, which also suggested a *strong stellar wind*. No such emission was observed previously. To fit the profiles of chromospheric lines and their fluxes, Dupree et al. (1992) computed the models of the supergiant's atmosphere and stellar wind provided *the presence of a constant magnetic field* of 10 G and the Alfvén wave energy flux for the cases of slow (115 km s−1) and fast (150 km s−1) wind and a temperature of 66 000 K. They showed that a rapid acceleration of the stellar wind should occur at a distance of 1.2R_*. Eaton (1995) demonstrated a distinct knifelike Hα profile obtained on August 20, 1992. A similar asymmetric profile with the analysis of the line bisector obtained on July 1, 1993, is mentioned by Usenko (2017). This allowed him to argue that there is an *extended envelope* around the supergiant. As a bright object, α Aqr has many photometric and spectroscopic observations. Its atmospheric parameters and chemical composition were determined in more than ten papers (Teff in the range 5091–5325 K, log g from 1.15 to 1.66, [Fe/H] from +0.03 to +0.31 dex), but the projected rotational velocity v sin i is 8 kms−1 (Bernacca and Perinotto 1970) and 10.5 km s−1 (Lubimkov et al. 2012). According to these authors, at a mass of 6.5 $M_\odot$ the lithium abundance in the supergiant's atmosphere is less than +0.9 dex in both LTE and non-LTE calculations. The object is not only bright IR source (IRAS 22032-0033; IRC +00513) but also has one of the largest IR excesses among the yellow nonvariable supergiants at wavelengths of 12, 25, and 60 μm (Deasy 1988). The stellar magnetic field is 0.47 $\pm$ 0.36 G (Grunhut et al. 2010). Parsons and Bouw (1971) estimated the star's radius to be 129 $R_\odot$, its absolute magnitude to be $MV = -5^m.4$, and

its mass to be 8.1 ± 1.1$M_{_}$. Based on a spectroscopic analysis, Schmidt (1972) gives $MV = -4\overset{m}{.}5$. Based on the oxygen 7771–7774 Å triplet lines, Kovtyukh et al. (2012) give $MV = -3\overset{m}{.}41$; according to Usenko (2017), the estimated absolute magnitude is $-3m.23$ and the radius and distance are 48 $R_{\odot}$ and 165 pc, respectively.

Radial Velocity Estimates

According to the CDS database, the radial velocity of α Aqr was determined from 1908 to 1974 (108 estimates in 12 publications), except for the estimate published in Usenko (2017). The radial velocity estimates differ: from +3.50 ± 0.30 (Buscombe and Kennedy 1968) to +7.80 ± 0.30 km s^{-1} (Griffin and Gunn 1974). All these papers, with the exception of Buscombe and Kennedy (1968), give only the radial velocity estimates without specifying the time at which they were obtained. The latter paper is interesting in that it shows how the radial velocity changes from +3.50 ± 0.44 to +6.20 ± 0.44 km s^{-1} almost in one day. Therefore, a suspicion about a possible variability of the supergiant arises.

Thus, we set the following goals.

(1) To carry out an archival search for previously obtained spectra of the supergiant, preferably with a high resolution, since α Aqr is a bright object and is often used as a spectroscopic standard.

(2) To perform a spectroscopic monitoring of the supergiant to determine its radial velocities in an effort to find possible manifestations of its variability.

(3) To estimate the radial velocities from hydrogen and metal absorption lines based on all the available spectra and to determine the effective temperatures.

(4) To assess the behavior of hydrogen and metal absorption lines to detect spectroscopic manifestations of the circumstellar envelope.

OBSERVATIONS AND PRIMARY REDUCTION

To solve the problem, we used the following.

(1) Two spectra taken in 1997 and 2003 with the 1.9-m telescope at the Haute Provence Observatory (France) (Elodie) using a spectrograph with a resolution $R \approx 42\,000$ in the wavelength range 4000–6790 Å and an S/N ratio of ∼100 (Moultaka et al. 2004).

(2) Two spectra taken in 2005 with the 1-m telescope at the Ritter Observatory (RO; Toledo, Ohio, USA) using a spectrograph with a resolution $R \approx 26\,000$ in the wavelength range 5283–6595 Å (nine spectral orders, each with a length of 70 Å) and an S/N ratio of ∼100. (3) Sixteen spectra taken in September– December 2016 with the 0.81-m TCO telescope (North Carolina, USA) using an echelle spectrograph with a resolution $R \approx 12\,000$ in the wavelength range

4250–7880 Å; the S/N ratio is ≈250 in the blue region (near Hβ) and ≈150 in the red region (near Hα). One spectrum (September 13, 2016) was taken with the 0.5-m telescope at the Amateur Observatory Kernersville (OK; near Winston-Salem, North Carolina, USA) equipped with the same spectrograph. Thus, the mean S/N ratio is 150–200, given that most of the lines used in our analysis were in the range 4900–6800 Å.

Table 1. Radial velocities determined from the metal lines for the archival spectra

Spectrum	HJD 2450000+	RV, km s−1								
		B	σ	NL	C	σ	NL	R	σ	NL
ELODIE 19970823	0684.4999	+2.78	1.14	54	+7.08	0.78	609	+13.12	2.12	64
ELODIE 20031005	2918.2650	+3.62	0.99	66	+7.03	0.77	576	+12.62	2.12	68
RO 20051004	3647.5924	+0.21	1.23	45	+6.46	1.89	162	+13.37	1.72	41
RO 20051020	3663.5901	+2.98	1.29	36	+7.46	1.42	164	+13.26	1.85	57

NL is the number of lines, B is the velocity from the blue line component, C is the velocity from the main line component, R is the velocity from the red line component.

Table 2. Radial velocities determined from the hydrogen lines for the archival spectra

Spectrum	Hα, kms^{-1}		Hβ, $km\ s^{-1}$		Hγ, km^{s-1}	
	B	C	R	R4	C	R
ELODIE 19970823	-2.57	+7.52	+28.84	+16.45	+9.56	+16.19
ELODIE 20031005	+6.73	+10.51	+22.39	+7.44	+8.79	+16.45
RO 20051004	+2.12	+13.32	+23.87	-	-	-
RO 20051020	+2.72	+11.05	+22.42	+50.25	-	-

B is the velocity from the blue Hα component;C is the velocity from themain line component,R is the velocity from the red component of the Hα, Hβ, Hγ lines.

We estimated the S/N ratio from the continuum and smoothed all spectra by a cubic polynomial before the reduction (this procedure is provided by an option in the DECH 30 software package; Galazutdinov 2007). The quality of the spectra can be estimated from Figs. 1–6. Tables 1–3 give information about the archival spectra: the mid-exposure heliocentric Julian date HJD and the radial velocity estimates from the metal (with the errors and the number of lines, respectively), hydrogen, and Na I D lines. Tables 4 and 5 provide similar information for the TCO spectra.

We described in detail the full process of obtaining the TCO spectra and reducing the CCD images in Usenko et al. (2016, 2017).

We reduced the spectra using the DECH 30 software package (Galazutdinov 2007), which allows the radial velocities to be measured by the cross-correlation and parabolic fitting methods. The accuracy of Vr measurements is 1–2.5 km $^{s-1}$.

Table 3. Radial velocities determined from the Na I D sodium doublet lines for the archival spectra

Spectrum	Na I (5889 Å), km s^{-1}		Na I (5895 Å), km s^{-1}	
	B	C	B	C
ELODIE 19970823	+3.54	+7.62	+4.02	+7.51
ELODIE 20031005	+2.51	+7.06	+2.48	+8.51
RO 20051004	-1.69	+7.32	-	+3.68
RO 20051020	-	+8.40	-	+7.24

B is the velocity from the blue line component, C is the velocity from the main line component.

The effective temperatures Teff were determined by a method based on the depth ratios of selected pairs of spectral lines most sensitive to the temperature (Kovtyukh 2007). This method provides an internal accuracy of Teff determination ∼10−30 K (the error of the mean).

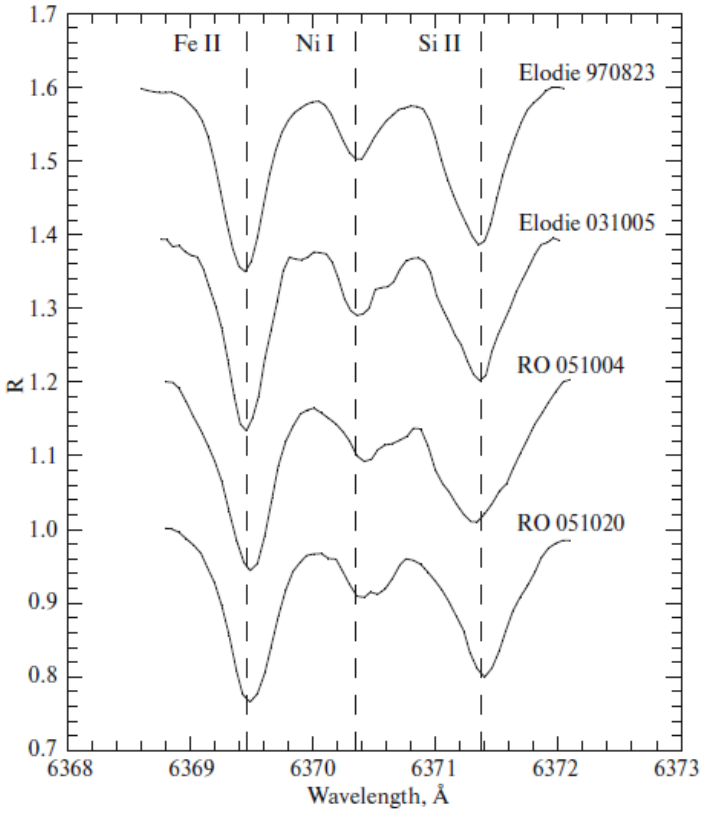

Fig. 1. Profiles of the Fe II 6369.460 A˚ (χlow = 2.89 eV), Ni I 6370.350 Å (χl_{ow} = 3.54 eV), and Si II 6371.370 Å (χ_{low} =8.12 eV) absorption lines in the archival spectra. The vertical dashed lines are the laboratory wavelengths for these elements.

SPECTROSCOPIC PECULIARITIES OF THE SUPERGIANT AND ITS RADIAL VELOCITY ESTIMATES

Usenko (2017) noticed an asymmetry of the Hα core (the so-called knifelike profile) and an asymmetry of the Na I D line profiles in the supergiant's spectrum taken in 1993 with a relatively low resolution, R = 15 000. At the same time, the remaining metal absorption lines showed nothing unusual, except for a few lines divided into two groups: with radial velocities less than 6 and more than 11 km s^{-1}. However, these lines in the high-resolution spectra from the archive (Elodie and RO) clearly show the presence of blue (B) and red (R) components, not only of neutral atoms but also of ions (Fig. 1). As can be seen from Table 1, these components are grouped near the mean values of 2–3 km s−1 (B) and 12–13 km s−1 (R) inmuch the same way as in the case of the 1993 spectrum. The number of B components is 7–10% of the number of lines used, while the number of R components is 9–10%. It should be noted that these components are more prominent in weaker lines (Fig. 2) than in strong ones (Fig. 3). Judging by the archival spectra, the appearance and presence of components differ in the time interval 1997–2005. The radial velocities determined from the metal lines show insignificant variations within the error limits, the mean value over this period (1997–2005) is +7.10 ±0.97 km s−1 (Fig. 4b). This estimate in 1993 was +7.54 ± 1.35 km s−1 (Usenko 2017). The values of *T*eff for all archival spectra differ insignificantly, and the mean estimate is 5290 ± 49 K.

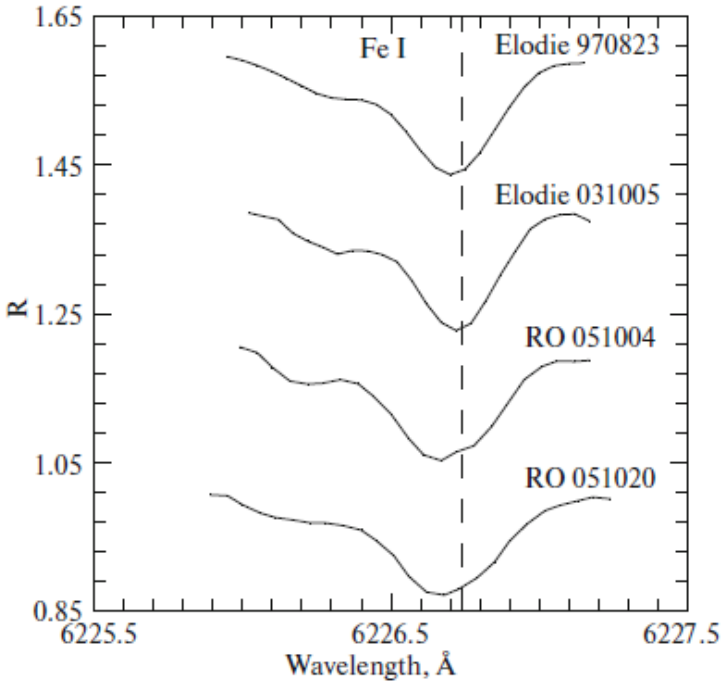

Fig. 2. Profile of the Fe I 6226.736 Å absorption line (χ_{low} = 3.88 eV) in the archival spectra. The vertical dashed line is the laboratory wavelength for this element.

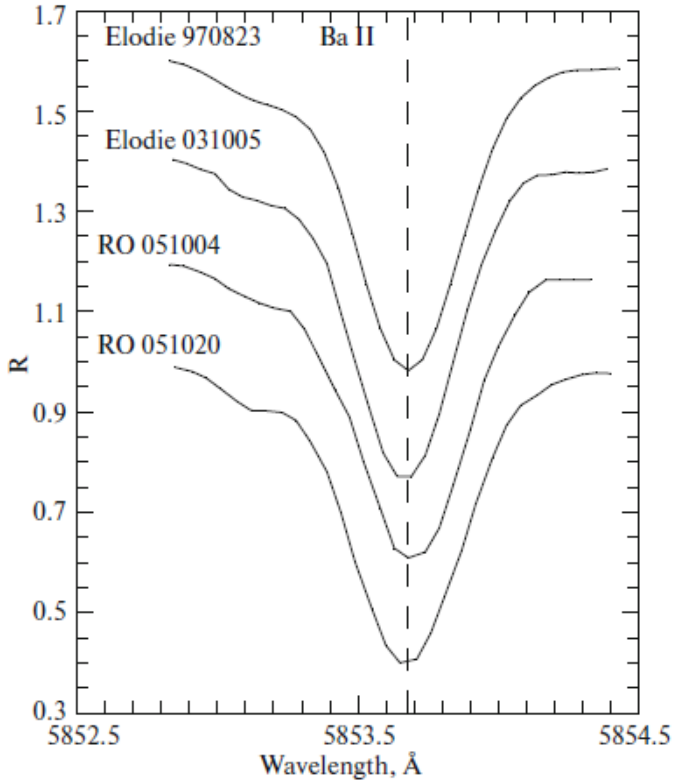

Fig. 3. Profile of the Ba II 5853.668 absorption line (χ_{low} = 0.60 eV) in the archival spectra. The vertical dashed line is the laboratory wavelength for this element.

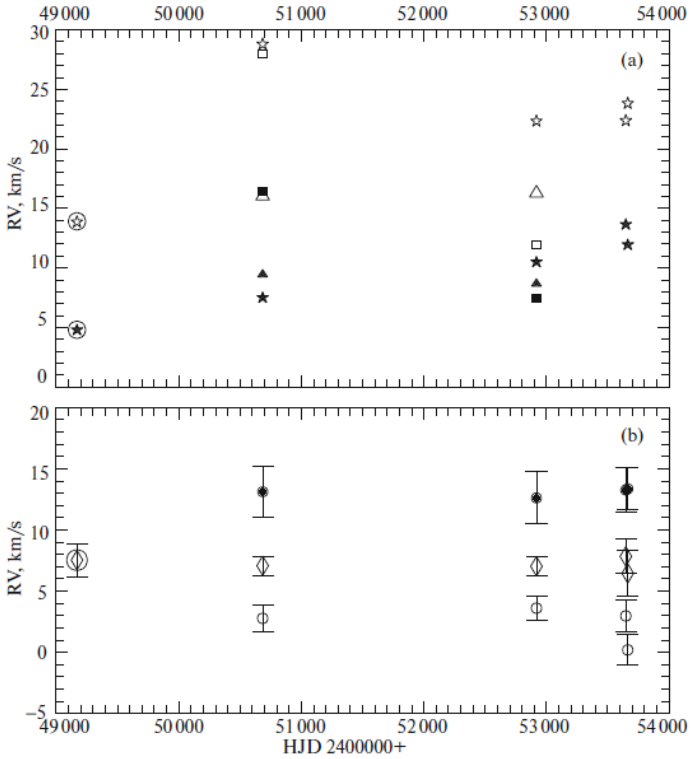

Fig. 4. Radial velocity estimates for the archival spectra. (b) The diamonds are the main components of the metal lines, the open circles are the B components, and the filled circles are the R components. The diamond in a circle is the estimate based on the 1993 spectrum from Usenko (2017). (a) The filled five-point stars indicate the Hα line, the open five-point stars are the R components, the filled squares indicate the Hβ line, the open squares are the R components of the Hβ line, the filled triangles indicate the Hγ line, the open triangles are the R components of the Hγ line, and the stars in circles are the estimates based on the 1993 spectrum.

The hydrogen lines, especially Hα, show a similar multicomponent structure (Fig. 4a). The presence of telluric H_2O lines that can distort the profile shape should be noted here. This is especially true for the Hα profiles. It can be seen from Fig. 5 that the lines near 6564 Å make the largest contribution. The 6563.5 Å water line is much weaker than these lines and cannot affect significantly the shape of the R component to be discussed below. We first measured the radial velocities from the main (or central) component that corresponds to the laboratory wavelength, given the heliocentric correction. As can be seen from Fig. 5, B and R components are observed in Hα. Hβ and Hγ exhibit one R component each (only the Elodie spectra). The radial velocities measured from all components are listed in Table 2.

Both lines in the Na I D doublet (Fig. 6) are noticeably asymmetric and this asymmetry can be explained precisely by the presence of B and R components. For example, the B components are clearly identified for three spectra (except for the 5889.950 Å line in RO 051020), if they are considered relative to the main component (as with the Hα line). The B component for the 5895.920 Å line is noticeable only in the Elodie 970823 and 031005 spectra. The R components are also present in the sodium doublet lines in all spectra, but they are strongly blended and, therefore, were not used for the radial velocity measurements. As with the Hα line, we also paid attention to the presence of telluric H2O lines, primarily the H2O 5889.64 Å line, while the water lines near 5896.4 Å are fairly weak. The radial velocities measured from the main and B components are listed in Table 3.

Such a multicomponent structure is known to be typical for yellow variable Cepheid supergiants with a circumstellar envelope (Mathias et al. 2006; Usenko 2016). Usenko (2017) showed the radial velocity differences between the components of both Na I D lines to be 3.9 and 1.8 km s−1, respectively (we mean the differences between the main and B components). In our case, they are from 4 to 9 km s−1 (5889.950 Å line) and from 3.5 to 6 km s−1 (5895.920 Å line) (Fig. 7).

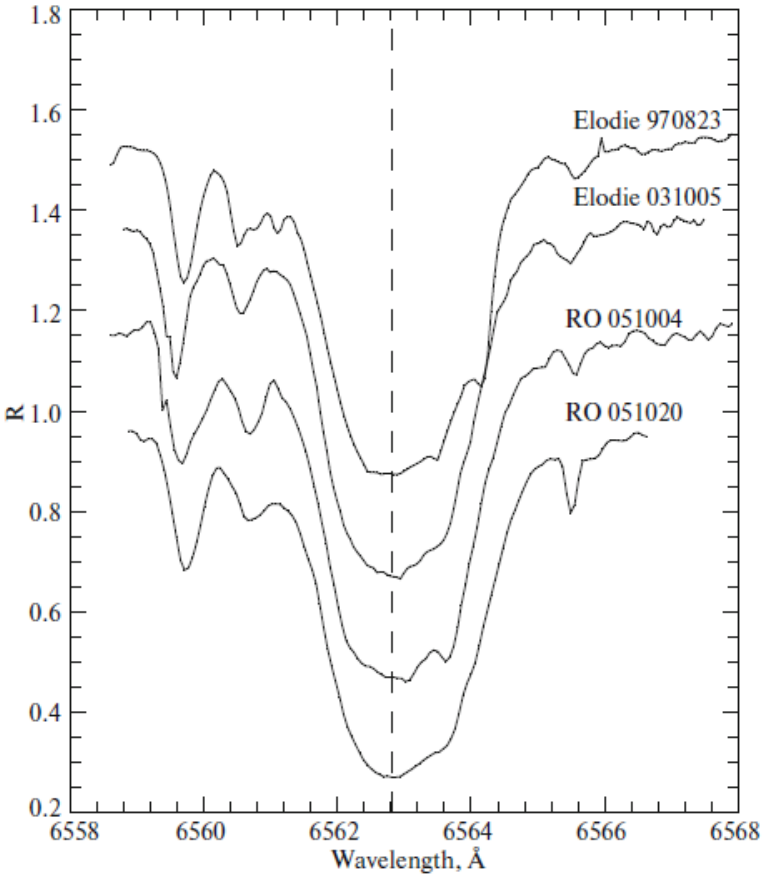

Fig. 5. Profiles of the Hα absorption line for the archival spectra. The vertical dashed line is the laboratory wavelength of the line.

OK and TCO Spectra

Despite the low resolution of the spectrograph, the metal absorption lines in the spectra also form three radial velocity groups: the blue one (B) with estimates from 2.5 to 5 kms^{-1}, the main one from7 to 8.4 km s^{-1}, and the red one (R) from12 to 14 kms^{-1} (Table 4). Obviously, there is good agreement with the data from the archival spectra; moreover, the percentage of blue and red lines is 7.5–11% and 9 to 15%, respectively. Since the velocities were determined from the line cores, the presence of B and R components in them is obvious. Judging by the data from Table 4 and Fig. 8b, the radial velocity showed insignificant variations within the error limits over the period of observations, with the R components exhibiting the largest variations. The mean radial velocity was +7.15 ± 1.35 km s^{-1}, and it virtually coincides with that for the archival data. Just as for the archival spectra, the effective temperatures show insignificant differences, and the mean estimate is *T*eff = 5185 ± 50 K.

Since no multicomponent structure of the sodium doublet lines is detected in these spectra, we obtained only one velocity estimate for each line. As can be seen from Table 5 and Fig. 8b, these estimates lie within the range of values for the metal lines, including the B and R components. On the whole, they are close to the estimates for the main components in the archival spectra.

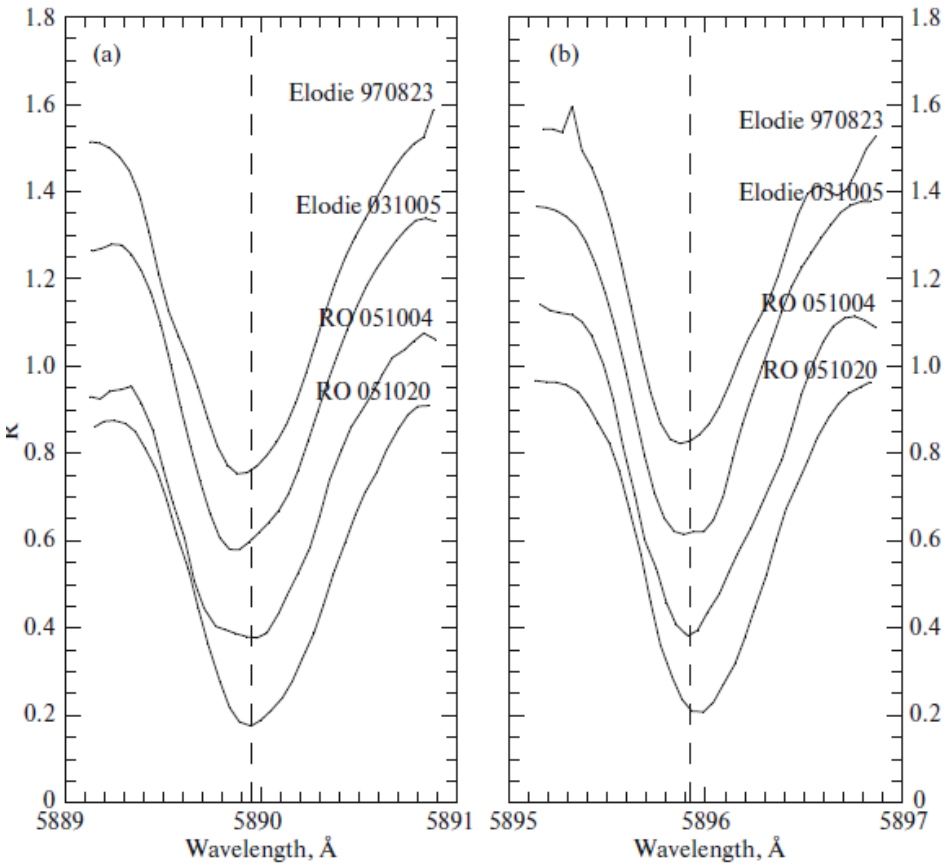

Fig. 6. Profiles of the Na I D I 5889.95 Å (a) and 5895.92 Å (b) absorption lines for the archival spectra. The vertical dashed lines are the laboratory wavelengths for sodium.

The R component is visible in theHα line (Figs. 9–11) due to the distinct asymmetry of the line core on the red side (knifelike profile). Despite the fact that the clearest separation into the main and R components is noticeable only in the 20161010 spectrum, the parabolic fitting method allows us to measure the radial velocities separately from each of them. Judging by the results from Table 5, the Hα line itself exhibits noticeable radial velocity variations in the range from 1 to 12 km s^{-1}, while the variations for the R component exceed 20 km s^{-1} (Fig. 8a). The radial velocities measured from the Hβ line vary by no more than 4.5 km s^{-1}; the presence of an R component can be judged only for six spectra, where a slight asymmetry is observed (Fig. 12). The radial velocities for Hγ are lower than those for Hβ approximately by 0.5 km s^{-1}, if the value for the 20160913 spectrum is excluded. In contrast to the archival spectra, no R component is observed in Hγ.

DISCUSSION

The four high-resolution archival spectra of α Aqr taken in 1997–2005 allowed us, first, to confirm the presence of an R component in the Hα core and to reveal the existence of analogous components in Hβ and Hγ, second, to confirm the multicomponent structure of the Na I D doublet line cores, and, third, most importantly, to detect the presence of B and R components in the metal absorption lines. This multicomponent structure is clearly seen in weaker lines and

manifests itself in the lines of both neutral atoms and ions, with different lower-level excitation potentials. The almost-three-month-long OK and TCO spectroscopic monitoring with a spectrograph with a relatively low resolution showed a noticeable presence and variability of the R component in the Hα core and a less noticeable one in Hβ as well as a good accuracy of the radial velocity estimates from the metal lines: the presence of B and R components was revealed from their distributions into the corresponding groups (from 2.5 to 5 kms^{-1} and from 12 to 14 km s^{-1}). The B and R components in the archival spectra are divided into approximately the same velocity groups. It should be noted here that, in both cases, the blue and red radial velocity estimates account for 20–25% of all the estimates obtained from the metal lines. The mean radial velocity estimates in both cases are virtually identical, which may be indicative of the absence of possible high-amplitude pulsations or manifestations of binarity. Judging by the monitoring results, the radial velocity estimates from the metal lines vary insignificantly, except for the 20160913 spectrum (Fig. 8b). A larger scatter of estimates is noticeable for the R components, but the errors for them are also twice as high. For the archival spectra there is a significant difference in velocities for the B components (Fig. 4b).

Table 4. Radial velocities determined from the metal lines for the OK and TCO spectra

Spectrum	HJD 2450000+	RV, km s−1								
		B	σ	NL	C	σ	NL	R	σ	NL
20160913	7645.5525	+5.15	0.98	47	+8.40	1.17	339	+12.99	1.38	65
20160924	7656.5339	+3.05	1.04	63	+7. 21	1.57	369	+13.50	1.75	90
20161001	7663.5624	+3.02	1.15	65	+7.22	1.33	380	+13.23	1.73	68
20161004	7666.5568	+3.33	0.97	70	+7.25	1.67	364	+12.89	1.68	87
20161010	7672.5412	+3.06	1.04	52	+7.09	1.17	359	+12.22	1.81	82
20161022	7684.5249	+2.96	0.98	57	+7.08	1.32	390	+13.64	2.36	65
20161028	7690.5622	+3.04	1.13	62	+7.20	1.41	395	+13.04	2.35	72
20161102	7695.5049	+2.96	0.99	65	+7.00	1.33	385	+13.37	2.24	69
20161104	7697.5439	+3.04	1.03	66	+7.02	1.26	370	+12.31	2.35	65
20161106	7699.5256	+3.07	0.96	68	+7.03	1.30	390	+13.02	2.31	69
20161110	7703.5025	+2.62	1.16	68	+6.96	1.39	385	+12.95	2.27	65
20161112	7705.4959	+2.56	1.12	66	+6.99	1.34	374	+13.73	2.55	54
20161115	7708.5203	+2.54	1.24	66	+6.88	1.33	386	+12.71	2.29	62
20161122	7715.5517	+2.66	0.78	69	+7.12	1.23	356	+11.82	2.10	58
20161126	7719.4718	+3.02	1.19	50	+6.97	1.23	340	+12.21	2.05	64
20161201	7724.4797	+2.76	1.08	64	+6.93	1.44	338	+13.20	2.17	58
20161209	7732.4662	+2.87	1.01	45	+7.18	1.39	340	+14.05	2.41	46

NL is the number of lines, RV (B) was measured from the blue line component, RV (C) was measured from the main line component, RV (R) was measured from the red line component.

Table 5. Radial velocities determined from the hydrogen and Na I D lines for the OK and TCO spectra

Spectrum	Hα, km s^{-1}		Hβ, km s^{-1}	Hγ, kms^{-1}	Na I D	
	C	R	C	C	5885 Å	5889 Å
20160913	+12.20	+31.88	+7.84	+15.94	+6.73	+10.37
20160924	+5.73	+26.59	+9.49	+7.96	+7.45	+8.95
20161001	+6.21	+24.02	+9.79	+9.96	+6.04	+8.49
20161004	+6.31	+26.62	+9.86	+9.97	+5.97	+8.69
20161010	+6.47	+24.60	+11.52	+11.75	+6.51	+7.77
20161022	+8.55	+23.34	+8.49	+9.69	+6.24	+7.23
20161028	+10.34	+18.99	+11.59	+12.23	+5.73	+7.53
20161102	+9.07	+25.66	+11.23	+11.57	+5.87	+7.52
20161104	+7.18	+17.27	+10.36	+11.36	+6.69	+7.59
20161106	+8.64	+15.81	+9.97	+10.48	+5.76	+6.82
20161110	+3.70	+23.05	+9.10	+9.78	+5.47	+7.16
20161112	+1.14	+14.03	+7.08	+10.16	+6.08	+6.64
20161115	+7.41	+9.52	+9.30	+10.41	+6.25	+7.06
20161122	+3.55	+23.80	+8.08	+9.53	+6.43	+7.18
20161126	+0.85	+15.65	+9.10	+11.80	+6.46	+7.25
20161201	+6.45	+17.60	+8.26	+9.89	+6.16	+6.92
20161209	+2.47	+19.66	+9.13	+10.21	+6.72	+7.65

RV (C) was measured from the main line component, RV (R) was measured from the red line component.

The most interesting fact revealed in this paper is the behavior of the H*α* core and its R components, namely their radial velocity estimates. As can be seen from our results and figures, the archival spectra show core velocity variations in the range 5–14 km s^{-1}, while the range for the R component is from 22 to 29 km s^{-1}. The scatters in velocities for H*β* and its R component are somewhat larger, while for H*γ* they are comparable to those for H*α*. If we consider the OK and TCO spectra, then here the H*α* core velocities vary in a slightly wider range (1–12 km s^{-1}), with a possible periodicity of these variations, ∼100 days, with abrupt sporadic changes being observed. This is more clearly seen from the velocities of the R component, where the variation amplitude is much larger, more than 20 km s^{-1} (9.5–32 km s^{-1}), and the velocity curve is virtually out of phase with the results for the Hα core. The radial velocity curve for the Hβ core closely follows that for Hα, but with much smaller sporadic variations. The velocity curve for the Hγ core is smoother with a similar amplitude.

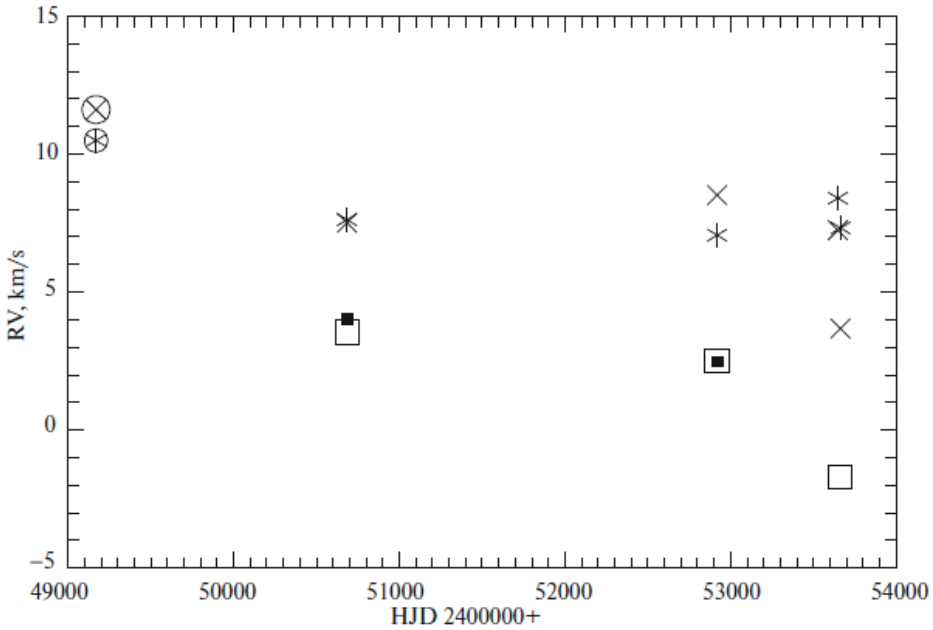

Fig. 7. Radial velocity estimates from the Na I D I 5889.95 and 5895.92 Å absorption lines for the archival spectra. The asterisks indicate the Na I 5889.966 Å line, the crosses indicate the Na I 5895.932 Å line, the open squares are the B components of the Na I 5889.966 Å line, the filled squares are the B components of the Na I 5895.932 Å line, the asterisk and the cross in circles are the estimates based on the 1993 spectrum.

As regards the Na I D doublet, no multicomponent structure of its lines is visible in the OK and TCO spectra, while the velocity estimates lie within or slightly exceed the estimation errors for the metal lines. Thus, we are dealing with the velocity estimates for the sodium lines forming in the supergiant's atmosphere. In contrast, this multicomponent structure is clearly seen in the archival spectra and, according to our measurements (Table 3 and Fig. 6), blended R components are present in both doublet lines, while the B components are clearly distinguished by their cores, although they are not present in all spectra. The estimates from the 1993 spectrum (Usenko 2017) were added to Fig. 7. In the figure we see how the velocities of the doublet components vary and differences in velocities between themain and B components, from 3.5 to 9 km s^{-1}, are noticeable. Unfortunately, since the R components of the doublet are strongly blended, we cannot estimate the same differences in velocities with the main components with a good accuracy. The study by Dupree (1986), where such a difference was estimated to be 25 km s−1, should also be recalled. Usenko (2017) described this fact as a manifestation of chromospheric activity and a strong stellar wind, a process conducive to the formation of an envelope around the supergiant and maintaining its presence.

The presence of blue and red absorption line components is typical for Cepheids with circumstellar envelopes. Using ζ Gem as an example, Usenko (2016) showed that the B components and some of the R components of metal absorption lines are formed through the κ-mechanism in the Cepheid atmosphere, while other R components, particularly the R component of the Hα core, correspond precisely to the envelope. In our case with α Aqr, the presence of distinct R components in the hydrogen lines and B components in the sodiumdoublet is a confirmation of the presence of a *circumstellar envelope* around the supergiant. Such

envelopes were detected first in long-period Cepheids and then in short-period Cepheids (Kervella et al. 2009) using IR photometry. Subsequently, it was concluded that these envelopes consist of a *heated part* maintained through the mass loss induced by pulsations, shocks, and stellar wind and a *cold dust component*, whose spectral lines resemble those of the interstellar medium (Gillet 2014). Usenko (2016) suggested that this envelope is initially formed around yellow supergiants *after the first dredge-up*, when the star ejects part of its mass. Subsequently, this mass forms an envelope whose existence is subsequently maintained through the processes mentioned above. Based on their studies of the Cepheid lCar, Nardetto et al. (2008) showed that the red asymmetry of the Hα line is *related to a continuous mass loss by th Cepheid*.

According to Usenko (2017), α Aqr has a mass of 4.7 $M_{\odot}$ and crosses the CIS not for the first time, i.e., it has already passed the first dredge-up. The presence of a strong stellar wind (Deasy 1988) from the supergiant also complements the picture explaining this asymmetry.

Judging by the IR excesses mentioned above, apart from the *heated part*, the supergiant also has a *cold dust component*. According to the calculations by Gillet (2014), such an envelope is located above the photosphere.

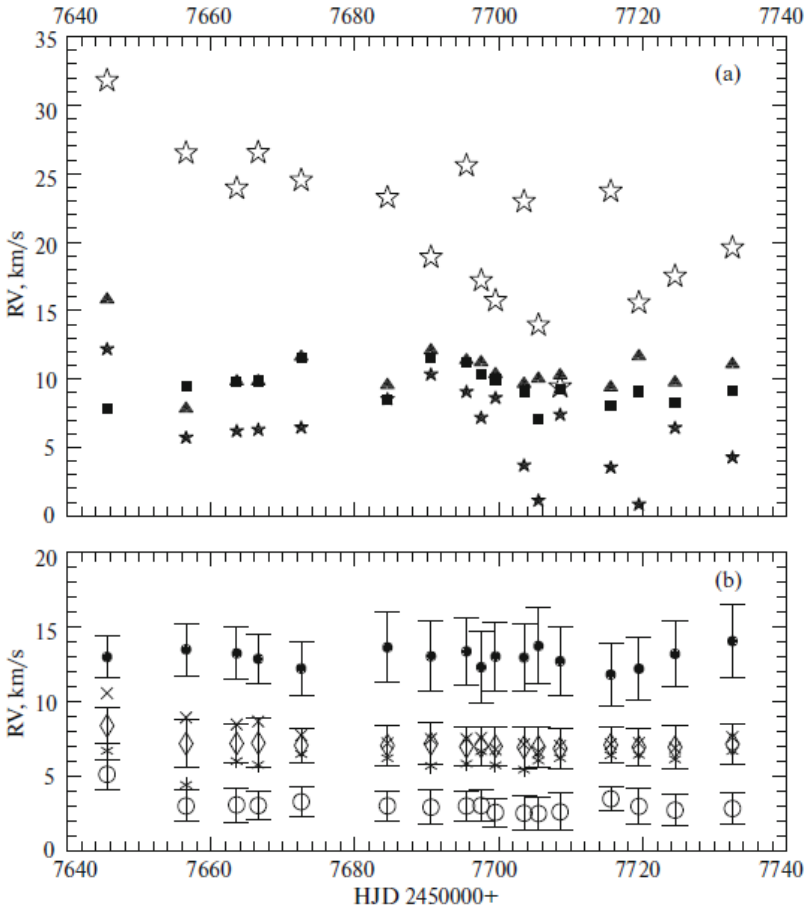

Fig. 8. Radial velocity estimates for the OK and TCO spectra. (b) The diamonds are the main components of the metal lines, the open circles are the B components, the filled circles are the R components, asterisks indicate the Na I 5889.966 Å line, the crosses indicate the Na I 5895.932 Å line. (a) The filled five-point stars indicate the Hα line, the open five-point stars are the R components, the filled squares indicate the Hβ line, the filled triangles indicate the Hγ line.

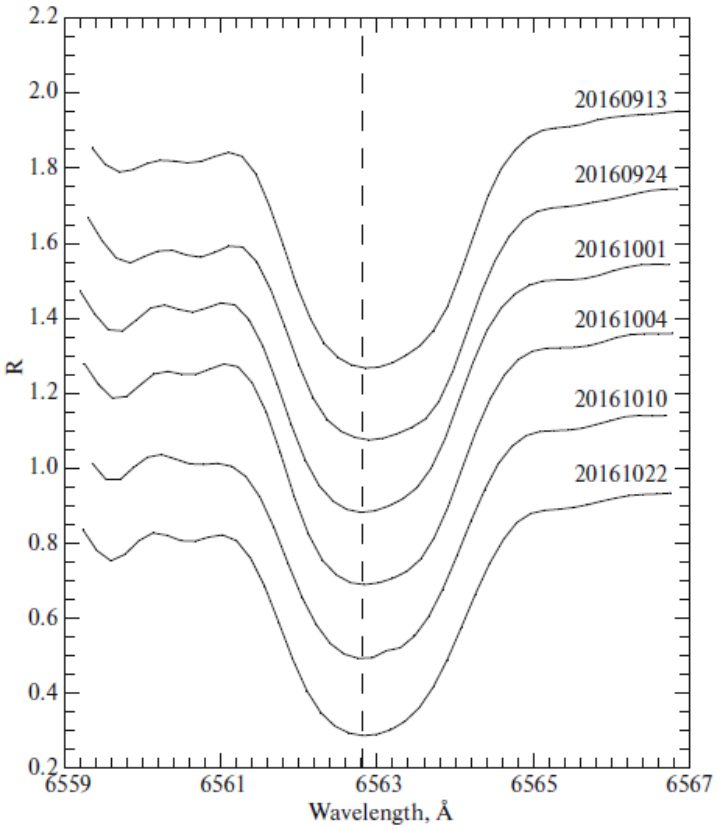

Fig. 9. Profiles of the Hα absorption line for the TCO spectra. Part 1. The vertical dashed line is the laboratory wavelength of the line.

The presence of B and R components in the metal lines as well as the strange variability in the hydrogen lines, particularly in the Hα line and its R component, can be explained as follows: α Aqr is at the red edge of the CIS (Usenko 2017), where, according to the theory of evolution, the pulsational activity is suppressed by convection in the stellar atmosphere. Some residual pulsational activity with a very small amplitude that takes place in the upper atmospheric layers, where, in particular, the main component of the Hα line is formed, probably manifests itself in this case. The oscillations in the upper atmospheric layers (a higher-density region) swing the stellar envelope (a lower-density region), as a result of which we observe radial velocity variations with a much larger amplitude in the latter. The sporadic radial velocity variations in the envelope can be associated with the chromospheric activity and stellar wind. Judging by the results of archival observations and our monitoring, the envelope around the supergiant is not a static structure but rather a very dynamic medium; this fact can force us to revise the classification of α Aqr as a nonvariable yellow supergiant. Furthermore, the results of our radial velocity monitoring for this star show that small telescopes with a relatively low spectral resolution but with a good accuracy of radial velocity determinations are efficient instruments in investigating bright yellow supergiants in the Galaxy.

Judging by our results, α Aqr confirms its reputation of a peculiar object and deserves more careful spectroscopic studies with a much higher resolution.

CONCLUSIONS

Our analysis of the available spectra led to the following conclusions.

(1) In the higher-resolution (Elodie and RO) spectra both blueshifted and redshifted components are observed in metal lines with different ionization potentials. The profiles and intensities of these components change with time, and they are most pronounced in weaker lines. The number of such components is 20–25% of the total number of lines used to analyze the spectra.

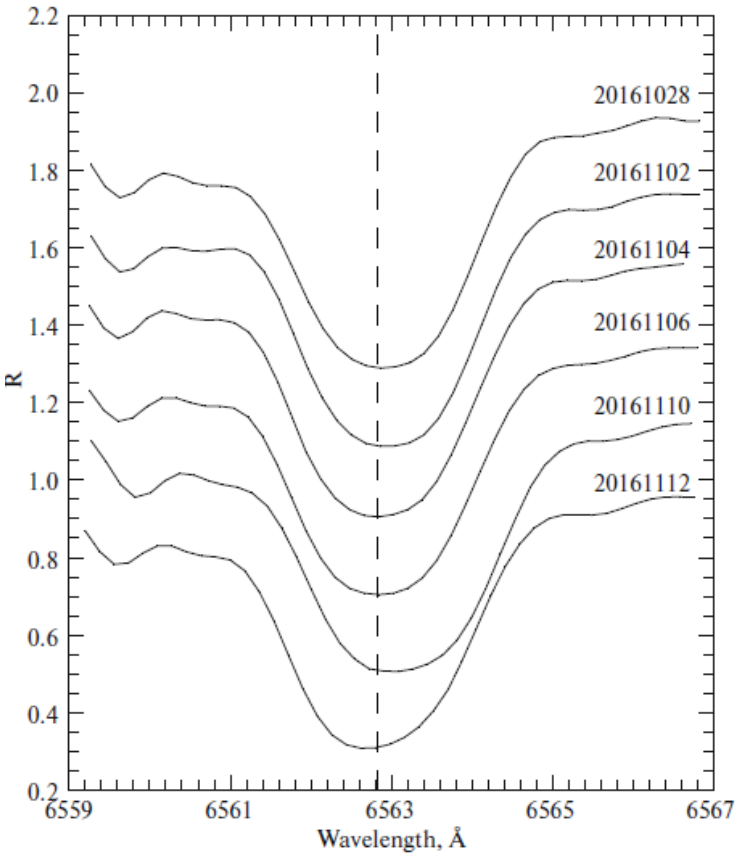

Fig. 10. Profiles of the Hα absorption line for the TCO spectra. Part 2. The vertical dashed line is the laboratory wavelength of the line.

(2) The OK and TCO spectra also exhibit such components, and their number is also 20–25% of the total number of lines used.

(3) Our radial velocity estimates for the B components are grouped in the ranges 2–3 (archival spectra) and 2.5–5 kms^{-1} (OK and TCO spectra), while for the R components these ranges are 12–13 and 12–14 km s^{-1}, respectively.

(4) The presence of R components is clearly seen in the cores of the hydrogen absorption lines, especially in Hα. Such an unusual behavior of the Hα and metal lines is typical for yellow supergiants with circumstellar envelopes.

(5) The multicomponent structure of the Na I D lines in the archival spectra also suggests the presence of a circumstellar envelope, both the *heated part* and the *cold dust component*, while the variations in the estimates of the component velocities over more than a decade are indicative of a change in chromospheric activity and stellar wind intensity. These processes also contribute to the formation and development of the circumstellar envelope.

(6) The spectroscopic estimates of Teff for the supergiant show no significant variations, and the mean value is about 5190 ± 50 K.

(7) The mean radial velocities determined from the metal lines show no variations within the measurement error limits, being +7.10 ± 0.97 (for the period 1997–2005) and +7.15 km s^{-1} (for the observing season of September–December 2016). The same can also be said about the estimates from the B and R components.

(8) The radial velocity estimates (OK and TCO spectra) from the hydrogen lines show noticeable variations. For example, they exceed 10 km s^{-1} for Hα and are smaller for Hβ and Hγ. These variations resemble periodic ones (∼100 days), with sporadic variations superimposed on them, but the number of estimates is clearly insufficient to claim that there is a clear periodicity.

(9) The radial velocity estimates (OK and TCO spectra) from the R component of the Hα core show the same variations resembling periodic ones, but with an amplitude that is twice as large and almost out of phase with the Hα variations and with the same sporadic variations.

(10) Since α Aqr is located at the red edge of the CIS, it can exhibit a residual pulsational activity with a very small amplitude whose manifestation can be, on the one hand, the presence of B and R components in the metal absorption lines and, on the other hand, radial velocity variability of the hydrogen lines, especially Hα that is formed in the upper atmospheric layers of the star.

(11) The large amplitude of radial velocity variations measured from the R component of the Hα core can be explained by the fact that the oscillations in the upper atmospheric layers (higher-density region) transfer their energy to the envelope (lower-density region), resulting in high-amplitude oscillations. The sporadic radial velocity oscillations of the hydrogen lines and their components can be caused by chromospheric activity and a change in stellar wind intensity. The supergiant's envelope is not a static structure but exhibits very active dynamics and, as has been mentioned above, consists of two parts, the *heated* and *cold dust* ones, and is located above the photosphere.

(12) The use of the 0.5-m OK telescope and the 0.81-m TCO telescope with a low-resolution spectrograph proved to be quite successful in searching for spectroscopic manifestations of the envelopes around yellow supergiants through an investigation of their hydrogen absorption lines and a possible variability through measurements of their radial velocities.

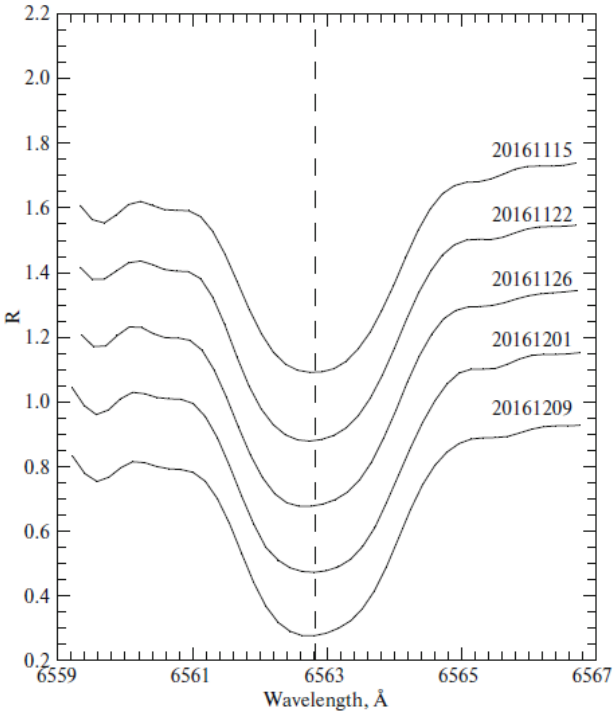

Fig. 11. Profiles of the Hα absorption line for the TCO spectra. Part 3. The vertical dashed line is the laboratory wavelength of the line.

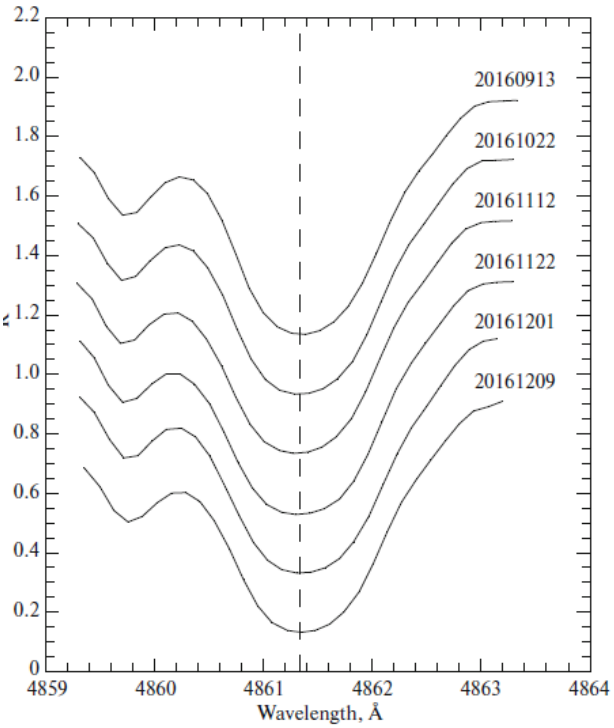

Fig. 12. Profiles of the Hβ absorption line with the R component for the TCO spectra. The vertical dashed line is the laboratory wavelength of the line.

(13) α Aqr confirms its reputation of a peculiar object and requires furthermore careful spectroscopic studies, preferably with a high resolution, and a possible revision of its classification as a nonvariable yellow supergiant in the CIS.

ACKNOWLEDGMENTS

This study was financially supported by the Swiss National Science Foundation SCOPES (project no. IZ73Z0152485). We are grateful to P. Prendergast from the Observatory Kernersville for the spectrum and to V.V. Kovtyukh for his help in preparing the paper.

REFERENCES

1. P. L. Bernacca and M. Perinotto, Contrib. Obs. Astron. Padova Asiago **239**, 1 (1970).

2. W. Buscombe and P. M. Kennedy, Mon. Not. R. Astron. Soc. **139**, 341 (1968).

3. H. P. Deasy, Mon. Not. R. Astron. Soc. **231**, 673 (1988).

4. A. K. Dupree, Ann. Rev. Astron. Astrophys. **24**, 377 (1986).

5. A. K. Dupree, B. A. Whitney, and E. H. Avrett, ASP Conf. Ser. **26**, 525 (1992).

6. J. A. Eaton, Astron. J. **109**, 1797 (1995).

7. J. D. Fernie and J. O. Hube, Astrophys. J. **168**, 437 (1971).

8. G. A. Galazutddinov, DECH 30 Package (2007). http//gazinur.com/DECH-sorftware.html

9. D. Gillet, Astron. Astrophys. **568**, A72 (2014).

10. R. F. Griffin and J. E. Gunn, Astrophys. J. **191**, 545 (1974).

11. J. H. Grunhut, G. A.Wade, D. A. Hanes, and E. Alecian, Mon. Not. R. Astron. Soc. **408**, 2290 (2010).

12. L. Hartmann, A. K. Dupree, and J. C. Raymond, Astrophys. J. **252**, 241 (1982).

13. D. R. Hollans and H. A. Beebe, Publ. Astron. Soc. Pacif. **88**, 934 (1976).

14. P. C. Keenan and R. C. McNeil,Astrophys. J. Suppl. Ser. **71**, 245 (1989).

15. F. Kervella, A. Mer´ and, and A. Gallenne, Astron. Astrophys. **498**, 425 (2009).

16. V. V. Kovtyukh, Mon. Not. R. Astron. Soc. **378**, 617 (2007).

17. V. V. Kovtyukh, N. I. Gorlova, and S. I. Belik, Mon. Not. R. Astron. Soc. **423**, 3268 (2012).

18. L. S. Lubimkov, D. L. Lambert, B. M. Kaminsky, Y. V. Pavlenko, D. B. Poklad, and T. M. Rachkovskaya, Mon. Not. R. Astron. Soc. **427**, 11L (2012).

19. P. Mathias, D. Gillet, A. B. Fokin, N. Nardetto, P. Kervella, and D. Mourard, Astron. Astrophys. **457**, 575 (2006).

20. J. Moultaka, S. A. Ilovaisky, P. Prugniel, and C. Soubiran, Publ. Astron. Soc. Pacif. **116**, 693 (2004).

21. D. J. Mullan and R. E. Stencel, Astrophys. J. **253**, 716 (1982).

22. G. T.O'Brien and D. L. Lambert, Astrophys. J. Suppl. Ser. **62**, 899 (1986).

23. I.Oznovich andD.M. Gibson,Astrophys. J. **319**, 383 (1987).

24. S. B. Parsons and G. D. Bouw,Mon. Not. R. Astron. Soc. **152**, 133 (1971).

25. D. Reimers, Astron. Astroph. **107**, 292 (1982).

26. E. G. Schmidt, Astrophys. J. **172**, 679 (1972).

27. R. E. Stencel and D. J. Mullan, Astrophys. J. **238**, 221 (1980).

28. I. A. Usenko, Astron. Lett. **42**, 393 (2016).

29. I. A. Usenko, Astron. Lett. **43**, 265 (2017).

30. I. A. Usenko, V. V. Kovtyukh, A. S. Miroshnichenko, and S. Danford,Odessa Astron. Publ. **29**, 100 (2016).

31. I. A. Usenko, V. V. Kovtyukh, A. S. Miroshnichenko, and S. Danford, Nauka Innov. **13**, 109 (2017).

32. O. C. Wilson and M. C. Vainu Bappu, Astrophys. J. **125**, 661 (1957).